

Scalable platform for qudit-based quantum computing using polar molecules

Soleh Kh. Muminov,^{1,2} Evgeniy O. Kiktenko,^{1,3} Anastasiia S. Nikolaeva,^{1,4} Denis A. Drozhzhin,^{1,4} Sergey I. Matveenko,^{1,5} Aleksey K. Fedorov,^{1,4} and Georgy V. Shlyapnikov^{1,6,7}

¹*Russian Quantum Center, Skolkovo, Moscow 121205, Russia*

²*Moscow Institute of Physics and Technology, Institutsky lane 9, Dolgoprudny, Moscow region, 141700, Russia*

³*Department of Mathematical Methods for Quantum Technologies,*

Steklov Mathematical Institute of Russian Academy of Sciences, Gubkina St. 8, Moscow 119991

⁴*National University of Science and Technology “MISIS”, Moscow 119049, Russia*

⁵*L. D. Landau Institute for Theoretical Physics, Chernogolovka 142432, Russia*

⁶*Université Paris-Saclay, CNRS, LPTMS, 91405 Orsay, France*

⁷*Van der Waals-Zeeman Institute, Institute of Physics, University of Amsterdam, Science Park 904, 1098 XH Amsterdam, The Netherlands*

We propose a model of a scalable qudit-based quantum processor that uses rotational degrees of freedom of polar molecules. Entangling gates between qudits are implemented via moving molecules in optical traps by exploiting dipole-dipole interactions to mediate coherent coupling. We develop encoding schemes that map single qubits ($d = 2$) into qudits of dimensions $2 \leq d \leq 5$, and pairs of qubits into higher-dimensional qudits with $d = 4, 5$. This approach enables the realization of a universal set of quantum gates. In particular, we exploit additional levels that are present in the $d = 3$ and $d = 5$ qudits, which allows one to simplify the decomposition of multiqubit gates. We then analyze the relevant experimental parameters to realize our schemes with SrF and $^{87}\text{Rb}^{133}\text{Cs}$ molecules. The proposed approach offers a promising route towards scalable and versatile quantum information processing with multilevel systems, which can be potentially realized using currently available experimental facilities.

I. INTRODUCTION

Recent progress in quantum information technologies has led to significant interest in the use of qudits (multilevel quantum systems) in view of their potential to enhance the efficiency of the execution of quantum algorithms [1–4] and error correction schemes [5–11]. Various quantum algorithms can be implemented in a more efficient manner with qudits (for review, see Ref. [12]) due to the fact that, first, a single qudit can be presented as a set of qubits [13–15] and, second, additional levels of qudits can be used as ancillas for simplifying the realization of multiqubit gates, such as the Toffoli gate [16–20]. The combination of these approaches may lead to a substantial reduction in circuit depth [12], which is of special interest for the current generation of noisy intermediate-scale quantum devices (NISQ) [21], where both the number of qubits and the fidelities of the gates are limited.

Among various physical systems studied for qudit implementations [22–30], polar molecules have emerged as a particularly promising platform [31]. Recent progress in experiments with cold polar molecules [32–37] has opened opportunities to use them in quantum computing [38–42] and metrology [43–48]. A particular feature of such systems is the possibility of controlling and manipulating the occupation of energy levels, in particular by using strong, tunable dipole-dipole interactions [31, 38, 40]. The rotational, vibrational, and electronic degrees of freedom inherent to these systems allow precise quantum state manipulations by external electromagnetic fields. Notably, rotational states present exceptional advantages for qudit encoding, as they exhibit long coherence times due to isolation from environmental decoherence channels. Fur-

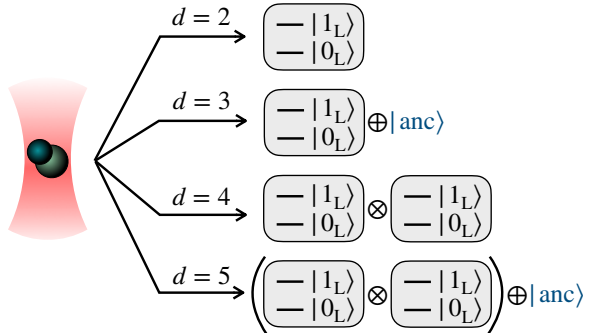


FIG. 1. Encoding schemes for qubits within the internal state space of a single molecular dipole, as explored in this work. The presented schemes utilize various dimensions (d) of the Hilbert space. The $d=2$ scheme employs a standard qubit encoding within the molecular states. A three-level system ($d=3$) is proposed, where two levels encode a qubit, and the third one serves as an ancilla for simplifying multi-qubit gate decomposition. Furthermore, a four-level encoding ($d=4$) enables the encoding of two qubits within a single molecule. Finally, a five-level scheme ($d=5$) is introduced, accommodating two qubits and an ancilla level, mirroring the functionality of the $d=3$ scheme.

thermore, permanent electric dipole moments characteristic of heteronuclear molecules provide a mechanism for establishing strong intermolecular couplings, which is a critical requirement for scalable quantum system architectures [38, 49, 50]. Experimental progress in laser cooling techniques [51] and optical confinement of ultracold molecular ensembles [52, 53], has significantly advanced

the prospects for practical realization of dipole-mediated quantum information processing.

In this work, we develop a scheme for universal qubit-based quantum computing using rotational levels of individual ultracold polar molecules confined in optical tweezer arrays, treating each molecule as a qubit or qudit of dimension $d = 3, 4, 5$ (see Fig. 1). The computational space is encoded in the subset of rotational levels: (i) encoding qubits in two-level subspaces; (ii) utilizing three-level subspaces to include an auxiliary level that simplifies multiqubit gate decompositions such as Toffoli gates; (iii) employing four-level subspaces to encode two qubits per molecule; and (iv) exploiting five-level subspaces to encode two qubits plus an auxiliary level for streamlined implementation of complex multiqubit operations. Although higher-dimensional encodings introduce additional experimental complexity, they offer enhanced flexibility and efficiency in the execution of quantum algorithms.

The key result of our work is the construction of a universal gate set that includes both single-qubit rotations and two-qubit entangling gates, the latter acting on qubits encoded within the same molecule or for different molecules [Fig. 2(a)]. To realize entangling gates between molecules, we propose a physically intuitive scheme based on dynamically bringing a pair of molecular tweezers to a close proximity (thus increasing the molecular dipole-dipole interaction) and then separating them again [Fig. 2(b)]. We numerically simulate the characteristics of this process for SrF and $^{87}\text{Rb}^{133}\text{Cs}$ molecules to validate the feasibility of our proposal. Importantly, our approach does not require exponential growth of the dimension of qudits with increasing circuit width, in contrast to previous proposals [31, 54, 55], where many qubits are embedded in a single large-dimensional qudit. Instead, we achieve scalability by increasing the number of molecules (qudits) while keeping the dimension of each qudit fixed. By scaling the computational Hilbert space based on the number of particles instead of exponentially increasing the qudit dimension, our approach becomes more flexible for implementing complex quantum algorithms. We expect that the combination of (i) multilevel encoding in molecular rotational states allowing efficient qudit construction, (ii) long coherence times characteristic of these rotational states, and (iii) our scalable universal gate architecture incorporating entangling operations between molecules makes this platform a highly promising candidate for scalable quantum computing.

The paper is organized as follows. In Sec. II we present a comprehensive examination of rotational-state manifolds in diatomic polar molecules as a foundation for qudit encoding. This section further elucidates the mechanisms by which dipole-dipole interactions may be used to generate entanglement between adjacent qudit systems. In Sec. III, we develop encodings for qudits with dimensions $d = 2, 3, 4$, and 5, and construct universal gate sets for each encoding. Finally, we summarize our results and conclude in Sec. IV.

II. OPERATING WITH DIPOLE-BASED QUUDITS

We consider a system of identical heteronuclear diatomic molecules interacting with each other via dipole-dipole interaction (DDI). In the adiabatic approximation, neglecting spin effects, molecular energy levels can be classified as electronic, vibrational, and rotational levels [56]. Throughout our work, we assume that the molecules are in their electronic and vibrational ground states and in their low rotational states. We denote the rotational states of a single molecule by $|J, M_J\rangle$, where $J = 0, 1, \dots$ is the orbital quantum number and $M_J = -J, \dots, J$ is its projection. The rotational part of the Hamiltonian for a single molecule can be expressed as:

$$\hat{H}_{\text{rot}} = \sum_J E_{\text{rot}}(J) \sum_{M_J} |J, M_J\rangle \langle J, M_J|, \quad (1)$$

$$E_{\text{rot}}(J) = BJ(J + 1),$$

where B is the rotational constant.

In this work, we consider finite d -element subsets of the set of all possible rotational states $\{|J, M_J\rangle\}$ as computational states for a qudit. Single-qudit operations of the form

$$\hat{R}_{x(y)}^{QQ'}(\theta) = \exp\left(-i\hat{\sigma}_{x(y)}^{QQ'} \frac{\theta}{2}\right), \quad (2)$$

can be induced by resonant Rabi oscillations. Here $Q = (J, M_J)$, $Q' = (J', M'_J)$ are two distinct pairs of quantum numbers, θ is a Bloch sphere rotation angle, and

$$\begin{aligned} \hat{\sigma}_x^{QQ'} &:= |J, M_J\rangle \langle J', M'_J| + \text{h.c.}, \\ \hat{\sigma}_y^{QQ'} &:= -i |J, M_J\rangle \langle J', M'_J| + \text{h.c.} \end{aligned} \quad (3)$$

Next, we consider an implementation of the entangling operation between dipolar qudits. Consider a system of two molecules with time-dependent Hamiltonian

$$\hat{H}_{\text{sys}}(t) = \hat{H}_1 + \hat{H}_2 + \hat{V}[R(t)], \quad (4)$$

where $\hat{H}_1 = \hat{H}_{\text{rot}} \otimes \hat{1}$ and $\hat{H}_2 = \hat{1} \otimes \hat{H}_{\text{rot}}$ correspond to the internal Hamiltonians (1) of the first and second molecules, respectively (here $\hat{1}$ stands for the identity operator), \hat{V} represents the dipole-dipole interaction, and $R(t)$ is the intermolecular separation, which is treated as a time-dependent parameter. Initially, at time $t = 0$, the intermolecular separation is assumed to be large, and therefore the interaction energy \hat{V} can be neglected. To entangle the molecules, they are slowly brought together to a minimum separation and then moved again to a larger distance over time $t = \tau$. During this process, the DDI alters the population of the molecular states, thereby applying a two-qudit gate.

The time evolution of the system state $|\psi(t)\rangle$ is governed by the time-dependent Schrödinger equation. Consider the projection of $|\psi(t)\rangle$ onto the basis states of the

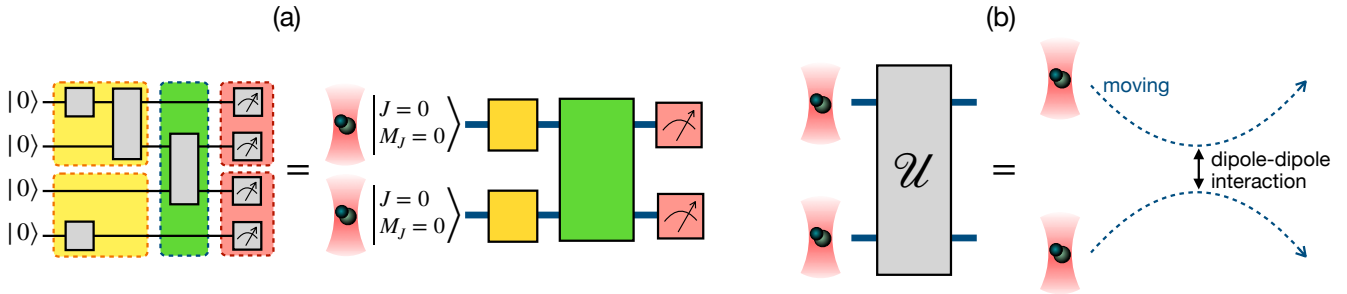


FIG. 2. (a) Schematic illustration of implementing a qubit-based quantum circuit using dipolar qudits, where each qudit encodes two qubits ($d = 4$). Single-qudit gates correspond to operations on qubits within the same molecule, while entangling gates between qubits in different qudits are realized via interactions between distinct molecules. (b) Conceptual depiction of the entangling gate between molecules, achieved by bringing two optical tweezers (and their respective dipoles) to close proximity to enable dipole-dipole interaction and then followed by their separation.

noninteracting molecules:

$$c_{\mathbf{Q}}(t) := (\langle J_1, M_{J_1} | \otimes \langle J_2, M_{J_2} |) e^{-iE_{\mathbf{Q}}t/\hbar} |\psi(t)\rangle, \quad (5)$$

where $\mathbf{Q} = (J_1, M_{J_1}; J_2, M_{J_2})$ is a multiindex of quantum numbers for two molecules and $E_{\mathbf{Q}} = E_{\text{rot}}(J_1) + E_{\text{rot}}(J_2)$. The time-dependent Schrödinger equation can then be expressed as [56]:

$$\frac{\partial c_{\mathbf{Q}}(t)}{\partial t} = \frac{1}{i\hbar} \sum_{\mathbf{Q}'} c_{\mathbf{Q}'}(t) V_{\mathbf{Q}\mathbf{Q}'}(t) e^{i(E_{\mathbf{Q}} - E_{\mathbf{Q}'})t/\hbar}, \quad (6)$$

where $V_{\mathbf{Q}\mathbf{Q}'}(t)$ is the matrix element of $\hat{V}[R(t)]$.

The slow approach and subsequent separation of molecules, governed by $R(t)$ for $t \in [0, \tau]$, allows us to neglect transitions between quantum states of different energies, in accordance with the adiabatic theorem. Consequently, the vibrational states remain unchanged, and

transitions occur solely between rotational states which have the same energies.

Using the spherical harmonic addition theorem, the DDI operator can be expressed as:

$$\begin{aligned} \hat{V}(\theta_1, \phi_1; \theta_2, \phi_2; R) \\ = \frac{d^2}{R^3} (\sin \theta_1 \sin \theta_2 \cos(\phi_1 - \phi_2) - 2 \cos \theta_1 \cos \theta_2), \end{aligned} \quad (7)$$

where d represents the magnitude of the dipole moment, R is the distance between the molecules, and the polar (azimuthal) angles θ_i (ϕ_i) specify the orientation of the i -th molecule. The matrix element of this operator takes the form:

$$\begin{aligned} V_{\mathbf{Q}\mathbf{Q}'}(t) &= \langle J_1, M_{J_1} | \otimes \langle J_2, M_{J_2} | \hat{V}[R(t)] | J'_1, M'_{J_1} \rangle \otimes | J'_2, M'_{J_2} \rangle \\ &= \frac{d^2}{R^3(t)} \sqrt{\frac{(2J_1 + 1)(2J_2 + 1)}{(2J'_1 + 1)(2J'_2 + 1)}} C_{1,0;J_1,0}^{J'_1,0} C_{1,0;J_2,0}^{J'_2,0} \left(\sum_{k=-1}^1 C_{1,k;J_1,M_{J_1}}^{J'_1,M'_{J_1}} C_{1,-k;J_2,M_{J_2}}^{J'_2,M'_{J_2}} + C_{1,0;J_1,M_{J_1}}^{J'_1,M'_{J_1}} C_{1,0;J_2,M_{J_2}}^{J'_2,M'_{J_2}} \right), \end{aligned} \quad (8)$$

where $C_{J_1,M_{J_1};J_2,M_{J_2}}^{J,M,J'}$ are the Clebsch-Gordan coefficients. It can be seen that there are the following selection rules: $\Delta J_1 = \pm 1$, $\Delta J_2 = \pm 1$, $\Delta M_{J_1} = 0, \pm 1$, $\Delta M_{J_2} = 0, \mp 1$.

To determine the evolution operator matrix, we solve the system of Eqs. (6) for a given time-dependent function $R(t)$ numerically. In our calculations we chose three

forms of $R(t)$:

$$\begin{aligned} R(t) &= \begin{cases} \alpha \cos\left(\frac{2\pi t}{\tau_1}\right) + \beta, & t \leq \tau_1 \\ \alpha + \beta, & t > \tau_1 \end{cases} \\ R(t) &= \begin{cases} -\frac{4\alpha t}{\tau_2} + \alpha + \beta, & t \leq \tau_2/2 \\ \frac{4\alpha t}{\tau_2} - 3\alpha + \beta, & \tau_2/2 < t \leq \tau_2 \\ \alpha + \beta, & t > \tau_2 \end{cases} \\ R(t) &= \begin{cases} \alpha \left(1 - \tanh\left(\frac{14t}{\tau_3} - 3\right)\right) + \beta - \alpha, & t \leq \frac{3\tau_3}{7} \\ \alpha \left(1 - \tanh\left(\frac{-14t}{\tau_3} + 9\right)\right) + \beta - \alpha, & \frac{3\tau_3}{7} < t \leq \frac{6\tau_3}{7} \\ \alpha(1 - \tanh(-3)) + \beta - \alpha, & t > \frac{6\tau_3}{7} \end{cases} \end{aligned} \quad (9)$$

where α and β are parameters such that $\beta + \alpha$ represents the initial intermolecular separation and $\beta - \alpha$ represents the minimum intermolecular separation, and τ_1, τ_2, τ_3 are tunable parameters.

For manipulations affecting only the rotational states of molecules (leaving the vibrational state unchanged), the characteristic timescale τ should significantly exceed \hbar/B . Furthermore, to ensure that the molecule remains confined within a single optical tweezer potential well, the center-of-mass kinetic energy acquired during the manipulation (approximately $m[(\alpha + \beta)/\tau]^2/2$) should be much smaller than the well depth U_0 . This condition leads to the requirement

$$\tau \gg \sqrt{\frac{m(\alpha + \beta)^2}{2U_0}} \equiv t_0. \quad (10)$$

As a goal for the optimization, we consider a maximization of the overlap between the resulting evolution operator, and an iSWAP-type gate acting in the subspace spanned by the set $\mathcal{Q}^{\otimes 2}$ with

$$\mathcal{Q} = \{|0, 0\rangle, |1, 0\rangle, |3, -3\rangle, |3, 0\rangle, |3, 3\rangle\}. \quad (11)$$

In the following section, \mathcal{Q} will be used as a source for the states that encode qubits. The target entangling gate, which acts in $\text{Span}(\mathcal{Q}^{\otimes 2})$, has the form

$$\begin{aligned} \mathcal{U} |1, 0\rangle \otimes |0, 0\rangle &= i |0, 0\rangle \otimes |1, 0\rangle \\ \mathcal{U} |0, 0\rangle \otimes |1, 0\rangle &= i |1, 0\rangle \otimes |0, 0\rangle \\ \mathcal{U} |J, M_J\rangle \otimes |J', M'_J\rangle &= |J, M_J\rangle \otimes |J', M'_J\rangle, \end{aligned} \quad (12)$$

where $|J, M_J\rangle |J', M'_J\rangle$ are taken from the set of 23 states $\mathcal{Q}^{\otimes 2} \setminus \{|0, 0\rangle \otimes |1, 0\rangle, |1, 0\rangle \otimes |0, 0\rangle\}$. One can think about the resulting \mathcal{U} as a direct sum of a two-qubit iSWAP gate in the subspace $\text{Span}(\{|0, 0\rangle, |1, 0\rangle\}^{\otimes 2})$ and identity in $\text{Span}(\{|3, -3\rangle, |3, 0\rangle, |3, 3\rangle\}^{\otimes 2})$. The target cost function for maximization is taken in the form:

$$\mathcal{F}_{\text{iSWAP}} = \frac{1}{25} |\text{Tr}(\mathcal{U}_{\mathcal{Q}}^{\text{phys}} \mathcal{U}^\dagger)|, \quad (13)$$

where $\mathcal{U}_{\mathcal{Q}}^{\text{phys}}$ is a projection of the solution of Eqs. (6) for given $R(t)$ on the 25-level subspace of $\mathcal{Q}^{\otimes 2}$. We also calculate the fidelity of the two-qubit identity gate

$$\mathcal{F}_{\text{id}} = \frac{1}{25} |\text{Tr}(\mathcal{I}_{\mathcal{Q}}^{\text{phys}})|, \quad (14)$$

where $\mathcal{I}_{\mathcal{Q}}^{\text{phys}}$ is a projection of the evolution operator for molecules remaining at rest at the distance $R(t) = \alpha + \beta$ during $t \in [0, \tau]$.

Numerical solutions of the system of differential equations (6) are obtained for SrF molecule in the $X^2\Sigma^+$ electronic state and $^{87}\text{Rb}^{133}\text{Cs}$ molecule in the $X^1\Sigma^+$ state. The values of the physical parameters are taken from [57–59]. The molecules are considered to be in a 10 mK deep potential well. The results are represented in Table I. In all cases, the fidelities $\mathcal{F}_{\text{iSWAP}}$ and \mathcal{F}_{id} are found to be close to 1, within the limits of numerical accuracy. Note that the obtained gate duration is much shorter than the coherence time of rotational levels, which ranges from microseconds to several tens of milliseconds [60–65].

TABLE I. Parameters of the $R(t)$ dependence obtained after numerical optimization. SrF and $^{87}\text{Rb}^{133}\text{Cs}$ were chosen as target molecules.

	SrF	$^{87}\text{Rb}^{133}\text{Cs}$
d, D	3.5	1.225
B, cm^{-1}	0.25	0.0163
initial distance $(\beta + \alpha), \mu\text{m}$	10	10
minimal distance $(\beta - \alpha), \mu\text{m}$	0.3	0.3
$t_0, \mu\text{sec}$	8.02	11.50
$\tau_1, \mu\text{sec}$	82.59	673.56
$\tau_2, \mu\text{sec}$	354.47	2893.64
$\tau_3, \mu\text{sec}$	60.72	495.73

III. QUANTUM COMPUTING WITH DIPOLAR QUDITS

In this section, we explore the potential use of the described system for running qubit-based quantum circuits. We propose several methods for encoding qubits in dipolar qudits and construct universal gate sets that are applicable to these encodings. We assume that the following operations can be performed: (i) single-qudit gates of the form (2) for states within the set \mathcal{Q} , (ii) entangling gate of the form (12), and (iii) measurement of a single qudit in the \mathcal{Q} basis. We further assume that the initial state of a qudit register is $|0, 0\rangle \otimes \dots \otimes |0, 0\rangle$, and that any leakage from \mathcal{Q} can be neglected for the purposes of this consideration. Below, we consider encoding schemes in d -dimensional subspaces of $\text{Span}(\mathcal{Q})$ for $d = 2, 3, 4$, and 5, as illustrated in Fig. 3.

A. Molecular dipole as qubit

We start with a straightforward encoding of a qubit in a 2-dimensional subspace:

$$|0, 0\rangle \leftrightarrow |0_L\rangle, \quad |1, 0\rangle \leftrightarrow |1_L\rangle. \quad (15)$$

(Hereinafter, we use subindex L to denote logical states of encoded qubits.)

Then single-qubit gates can be directly realized via $R_{x(y)}^{0,0,1,0}(\theta)$, while \mathcal{U} can be used as a two-qubit iSWAP gate:

$$\begin{aligned} \mathcal{U} |0_L\rangle \otimes |0_L\rangle &= |0_L\rangle \otimes |0_L\rangle, \\ \mathcal{U} |0_L\rangle \otimes |1_L\rangle &= i |1_L\rangle \otimes |0_L\rangle, \\ \mathcal{U} |1_L\rangle \otimes |0_L\rangle &= i |0_L\rangle \otimes |1_L\rangle, \\ \mathcal{U} |1_L\rangle \otimes |1_L\rangle &= |1_L\rangle \otimes |1_L\rangle. \end{aligned} \quad (16)$$

The inverse of the iSWAP gate with i replaced by $-i$ can be created by using a pair of Pauli Z gates $Z \otimes Z = \text{diag}(1, -1, -1, 1)$ before (or after) the iSWAP gate. Single-qubit Z can be obtained by applying $R_x^{\text{L}, A}(2\pi)$, where A denotes a level in \mathcal{Q} other than $|0, 0\rangle$ and $|1, 0\rangle$.

 = 1 qubit	 = 1 qubit + anc. state	 = 2 qubits	 = 2 qubits + anc. state
$ 0_L\rangle = \begin{pmatrix} J=0 \\ M_J=0 \end{pmatrix}$	$ 0_L\rangle = \begin{pmatrix} J=0 \\ M_J=0 \end{pmatrix}$	$ 0_L\rangle \otimes 0_L\rangle = \begin{pmatrix} J=0 \\ M_J=0 \end{pmatrix}$	$ 0_L\rangle \otimes 0_L\rangle = \begin{pmatrix} J=0 \\ M_J=0 \end{pmatrix}$
$ 1_L\rangle = \begin{pmatrix} J=1 \\ M_J=1 \end{pmatrix}$	$ 1_L\rangle = \begin{pmatrix} J=1 \\ M_J=1 \end{pmatrix}$	$ 0_L\rangle \otimes 1_L\rangle = \begin{pmatrix} J=1 \\ M_J=0 \end{pmatrix}$	$ 0_L\rangle \otimes 1_L\rangle = \begin{pmatrix} J=1 \\ M_J=0 \end{pmatrix}$
$ \text{anc}\rangle = \begin{pmatrix} J=3 \\ M_J=0 \end{pmatrix}$		$ 1_L\rangle \otimes 0_L\rangle = \begin{pmatrix} J=3 \\ M_J=-3 \end{pmatrix}$	$ 1_L\rangle \otimes 0_L\rangle = \begin{pmatrix} J=3 \\ M_J=-3 \end{pmatrix}$
		$ 1_L\rangle \otimes 1_L\rangle = \begin{pmatrix} J=3 \\ M_J=-3 \end{pmatrix}$	$ 1_L\rangle \otimes 1_L\rangle = \begin{pmatrix} J=3 \\ M_J=-3 \end{pmatrix}$
			$ \text{anc}\rangle = \begin{pmatrix} J=3 \\ M_J=0 \end{pmatrix}$

FIG. 3. A summary of the schemes for encoding a single or two qubits in a single dipole with $d = 2, 3, 4$, and 5 (columns from left to right), as discussed in the main text.

We also note that the controlled NOT (CNOT) gate can be realized by using two iSWAP gates with single-qubit operations [66].

B. Molecular dipole as qubit and ancillary level

The second approach extends the previous one by adding an ancillary logical level $|\text{anc}\rangle$:

$$|0,0\rangle \leftrightarrow |0_L\rangle, \quad |1,0\rangle \leftrightarrow |1_L\rangle, \quad |3,0\rangle \leftrightarrow |\text{anc}\rangle. \quad (17)$$

As in the previous case, the universal gate set can be constructed on the basis of single-qubit gates and iSWAP gate (16). At the same time, by surrounding \mathcal{U} with single-qudit gates P and P^\dagger , where

$$P := R_y^{0_L, \text{anc}}(-\pi) R_y^{0_L, 1_L}(\pi) \quad (18)$$

provides the following transformation:

$$P|0_L\rangle = |1_L\rangle, \quad P|1_L\rangle = |\text{anc}\rangle, \quad P|\text{anc}\rangle = |0_L\rangle, \quad (19)$$

and we can synthesize the operation in the following manner:

$$\text{iSWAP}^{0_L, \text{anc}} := (\mathbb{1} \otimes P) \mathcal{U} (\mathbb{1} \otimes P^\dagger) \quad (20)$$

which acts as follows:

$$\begin{aligned} \text{iSWAP}^{0_L, \text{anc}} |1_L\rangle \otimes |1_L\rangle &= i|0_L\rangle \otimes |\text{anc}\rangle, \\ \text{iSWAP}^{0_L, \text{anc}} |0_L\rangle \otimes |\text{anc}\rangle &= i|1_L\rangle \otimes |1_L\rangle, \\ \text{iSWAP}^{0_L, \text{anc}} |x_L\rangle \otimes |y_L\rangle &= |x_L\rangle \otimes |y_L\rangle \end{aligned} \quad (21)$$

for $|x_L\rangle |y_L\rangle \in \{|0\rangle, |1\rangle, |\text{anc}\rangle\}^{\otimes 2} \setminus \{|1_L\rangle |1_L\rangle, |0_L\rangle |\text{anc}\rangle\}$. This gate can be used to decompose a generalized N -qubit controlled-phase gate $C^{N-1}Z$:

$$\begin{aligned} C^{N-1}Z |1_L\rangle \otimes \dots \otimes |1_L\rangle &= -|1_L\rangle \otimes \dots \otimes |1_L\rangle, \\ C^{N-1}Z |x_L^1\rangle \otimes \dots \otimes |x_L^{N-1}\rangle &= |x_L^1\rangle \otimes \dots \otimes |x_L^{N-1}\rangle, \end{aligned} \quad (22)$$

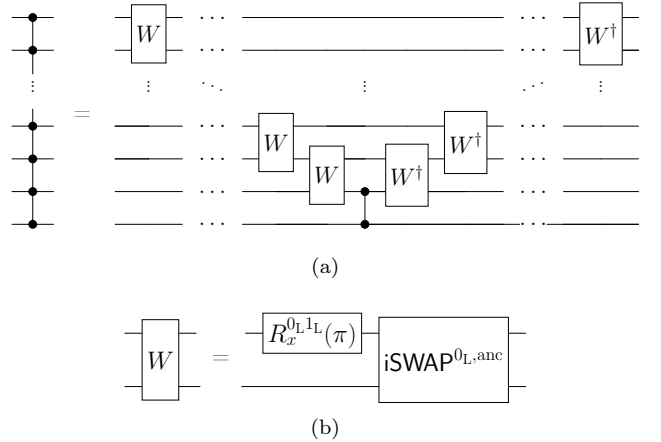


FIG. 4. (a) $C^{N-1}Z$ decomposition with $2N - 4$ W operations and two $\text{iSWAP}_{1L, \text{anc}}$ gates (for the implementation of CZ in the center of the scheme), when dipole is considered as a qutrit: qubit with ancillary state. (b) Definition of the operation W with iSWAP gate and single-qudit rotation.

where $\prod_{i=1}^N x_i \neq 1$ using $2N-2$ application of \mathcal{U} as shown in [67].

The idea of the decomposition shown in Fig. 4(a) is as follows. First, we note that the multiqubit gate in Eq. (22) applies the phase factor -1 to all N involved qubits if and only if they are in the state $|1_L\rangle^{\otimes L}$; otherwise, the state of the qubits remains the same. To decompose $C^{N-1}Z$, we introduce an operation W that acts on $N - 2$ pairs of qudits:

$$\begin{aligned} W|0_L\rangle \otimes |0_L\rangle &= |1_L\rangle \otimes |0_L\rangle, \\ W|0_L\rangle \otimes |1_L\rangle &= i|0_L\rangle \otimes |\text{anc}\rangle, \\ W|1_L\rangle \otimes |0_L\rangle &= |0_L\rangle \otimes |0_L\rangle, \\ W|1_L\rangle \otimes |1_L\rangle &= |0_L\rangle \otimes |1_L\rangle, \end{aligned} \quad (23)$$

and whose construction is shown in Fig. 4(b). The operator W is designed so that the bottom qubit remains

in the state $|1_L\rangle$ only when the inputs are in the state $|1_L\rangle \otimes |1_L\rangle$. Therefore, after the sequence of W operations in Fig. 4(a), if the lower qubit comes to the state $|1_L\rangle$, it implies that each qubit affected by the sequence was initially in the state $|1_L\rangle$. In this case, the application of a central controlled phase gate will add a -1 phase if and only if all qubits were in the $|1_L\rangle$ initial state. Finally, a series of uncomputation operations W^\dagger is applied to remove populations of all ancillary states $|\text{anc}\rangle$.

The use of iSWAP gate as a basic entangling operation makes the decomposition in Fig. 4(a) adaptive for arbitrary coupling map between dipoles (see [67] for more details). In particular, the depth $\mathcal{O}(\log N)$ of the decomposition circuit is achieved for a binary-tree coupling map. We also note that the multiqubit Toffoli gate can be obtained from the $C^{N-1}Z$ gate by applying a pair of single-qudit gates to the target before and after $C^{N-1}Z$.

C. Molecular dipole as two qubits

Next we consider encoding of a pair of qubits in a single 4-level dipole (ququart) according to the following mapping between qubit and qudit states:

$$\begin{aligned} |0,0\rangle &\leftrightarrow |0_L0_L\rangle, \\ |1,0\rangle &\leftrightarrow |0_L1_L\rangle, \\ |3,-3\rangle &\leftrightarrow |1_L0_L\rangle, \\ |3,3\rangle &\leftrightarrow |1_L1_L\rangle. \end{aligned} \quad (24)$$

All single-qubit gates and two-qubit gates for qubits embedded in the same qudit can be realized via local operations [68]. In particular, a single qubit gate u can be considered as a tensor product of the form $u \otimes 1$ or $1 \otimes u$, where 1 is the 2×2 identity acting on a neighboring, unaffected qubit that resides in the same qudit. These tensor products can then be straightforwardly decomposed into two-level operations. The entangling iSWAP gate acting on two qubits of the same qudit can be realized as $R_x^{(0_L1_L),(1_L0_L)}(-\pi/2)$.

Regarding entangling gates between qubits residing in different qudits, these can be constructed as follows. According to the mapping, the \mathcal{U} operation acts as

$$\begin{aligned} \mathcal{U}|0_L0_L\rangle \otimes |0_L1_L\rangle &= i|0_L1_L\rangle \otimes |0_L0_L\rangle, \\ \mathcal{U}|0_L1_L\rangle \otimes |0_L0_L\rangle &= i|0_L0_L\rangle \otimes |0_L1_L\rangle, \end{aligned} \quad (25)$$

and acts as the identity operator on the remaining $4^2 - 2 = 14$ levels of joint space of four qubits. One can see that this is a $|0_L\rangle^{\otimes 2}$ -controlled iSWAP gate, where the iSWAP operation is applied to the second and fourth qubits when the first and the third qubits are in the all-zero state [see Fig. 5(a)]. The realization of a standard iSWAP gate between qubits from distinct qudits is illustrated in Fig. 5(b). In this construction, the control pattern can be modified by applying single-qubit inversion gates as needed.

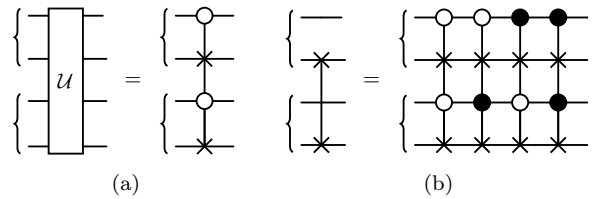


FIG. 5. (a) The scheme of the controlled iSWAP gate. (b) The synthesis of the CNOT gate between qubits from distinct qudits. Vertical braces denote qubits that belong to the same qudit. We note that the x symbols used here represent iSWAP rather than a standard SWAP operation, as is typically the case.

D. Molecular dipole as two qubits with joint ancillary level

A single 5-level dipole (ququint) can be considered as a pair of qubits with a joint ancillary level according to the following mapping of the states:

$$\begin{aligned} |0,0\rangle &\leftrightarrow |0_L0_L\rangle, \\ |1,0\rangle &\leftrightarrow |0_L1_L\rangle, \\ |3,-3\rangle &\leftrightarrow |1_L0_L\rangle, \\ |3,3\rangle &\leftrightarrow |1_L1_L\rangle, \\ |3,0\rangle &\leftrightarrow |\text{anc}\rangle. \end{aligned} \quad (26)$$

We note that mapping (26) in a 4-level subspace, which corresponds to the space of two qubits, is equal to mapping (24). Therefore, single-qubit gates and two-qubit gates, for all possible embeddings of qubits in qudit space, are implemented as it is described in section III C.

However, due to the presence of joint ancillary level we can efficiently decompose multiqubit gates [68]. In particular, generalized 4-qubit controlled phase gate C^3Z can be implemented with two successive applications of \mathcal{U} operations and single-ququint gates as it is shown in Fig. 6.

IV. CONCLUSION

We have developed a scalable qudit platform based on diatomic polar molecules, which is among the leading platforms for quantum technologies. Our approach uses rotational levels of the molecules with qudit dimensions $d = 2, 3, 4$ and 5 . A universal gate set has been proposed, and entangling gates between qudits are created relying on molecules moving in optical traps and exhibiting coherent couplings due to dipole-dipole interactions. Numerical simulations for SrF and $^{87}\text{Rb}^{133}\text{Cs}$ molecules have demonstrated the feasibility of this approach. Specifically, it has been shown that the gate times can be shorter than the coherence times of the rotational levels, which opens the way to realizing quantum algorithms with such systems. This scalable architecture

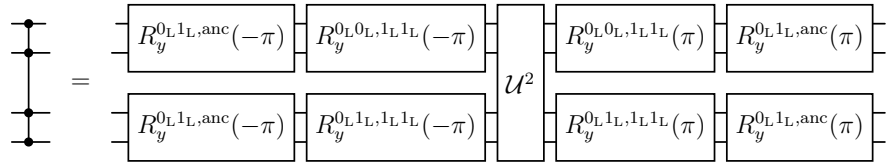


FIG. 6. C^3Z decomposition with \mathcal{U} operation and single-quint rotations.

offers a promising path towards robust and efficient quantum computation using ultracold polar molecules. Advantages of the proposed approach in experiments can be demonstrated by reducing the number of operations required to realize quantum algorithms, such as Grover's search and Bernstein–Vazirani algorithm.

ACKNOWLEDGEMENTS

We are grateful to A. V. Akimov and S. S. Straupe for fruitful discussions. The work of E.O.K. on designing the

universal gate set for dipole qubits was supported by the state assignment of the Ministry of Science and Higher Education of the Russian Federation (Section IIIA). The work of A.K.F. is supported by the Priority 2030 program at the NIST "MISIS" under the project K1-2022-027 (developing gate set for qubit pairs, encoded in dipole qudits; Section IIIC). The work of A.S.N. and D.A.D. was supported by RSF Grant No. 24-71-00084 (developing realization of multicontrolled-phase gate on dipole qudits; Sections IIIB and IIID).

[1] A. Muthukrishnan and C. R. Stroud Jr, *Physical review A* **62**, 052309 (2000).

[2] S. D. Bartlett, H. de Guise, and B. C. Sanders, *Phys. Rev. A* **65**, 052316 (2002).

[3] Z. Zilic and K. Radecka, *IEEE Transactions on computers* **56**, 202 (2007).

[4] V. Parasa and M. Perkowski, in *2011 41st IEEE International Symposium on Multiple-Valued Logic* (2011), pp. 224–229.

[5] E. T. Campbell, H. Anwar, and D. E. Browne, *Physical Review X* **2**, 041021 (2012).

[6] G. Duclos-Cianci and D. Poulin, *Physical Review A—Atomic, Molecular, and Optical Physics* **87**, 062338 (2013).

[7] E. T. Campbell, *Physical review letters* **113**, 230501 (2014).

[8] H. Anwar, B. J. Brown, E. T. Campbell, and D. E. Browne, *New Journal of Physics* **16**, 063038 (2014).

[9] R. S. Andrist, J. R. Wootton, and H. G. Katzgraber, *Physical Review A* **91**, 042331 (2015).

[10] F. H. Watson, E. T. Campbell, H. Anwar, and D. E. Browne, *Physical Review A* **92**, 022312 (2015).

[11] A. Krishna and J.-P. Tillich, *Physical review letters* **123**, 070507 (2019).

[12] E. O. Kiktenko, A. S. Nikolaeva, and A. K. Fedorov, *Reviews of Modern Physics* **97**, 021003 (2025).

[13] A. D. Greentree, S. G. Schirmer, F. Green, L. C. L. Hollenberg, A. R. Hamilton, and R. G. Clark, *Phys. Rev. Lett.* **92**, 097901 (2004), URL <https://link.aps.org/doi/10.1103/PhysRevLett.92.097901>.

[14] E. O. Kiktenko, A. K. Fedorov, O. V. Man'ko, and V. I. Man'ko, *Phys. Rev. A* **91**, 042312 (2015), URL <https://link.aps.org/doi/10.1103/PhysRevA.91.042312>.

[15] E. Kiktenko, A. Fedorov, A. Strakhov, and V. Man'ko, *Physics Letters A* **379**, 1409 (2015), ISSN 0375-9601, URL <https://www.sciencedirect.com/science/article/pii/S0375960115002753>.

[16] T. C. Ralph, K. J. Resch, and A. Gilchrist, *Phys. Rev. A* **75**, 022313 (2007), URL <https://link.aps.org/doi/10.1103/PhysRevA.75.022313>.

[17] A. Fedorov, L. Steffen, M. Baur, M. P. da Silva, and A. Wallraff, *Nature* **481**, 170 (2012), URL <https://doi.org/10.1038/nature10713>.

[18] L. B. Nguyen, N. Goss, K. Siva, Y. Kim, E. Younis, B. Qing, A. Hashim, D. I. Santiago, and I. Siddiqi, *Nature Communications* **15**, 7117 (2024).

[19] E. O. Kiktenko, A. S. Nikolaeva, P. Xu, G. V. Shlyapnikov, and A. K. Fedorov, *Physical Review A* **101**, 022304 (2020).

[20] A. S. Nikolaeva, I. V. Zalivako, A. S. Borisenko, N. V. Semenin, K. P. Galstyan, A. E. Korolkov, E. O. Kiktenko, K. Y. Khabarova, I. A. Semerikov, A. K. Fedorov, et al., *Phys. Rev. Lett.* **135**, 060601 (2025), URL <https://link.aps.org/doi/10.1103/p1z9-6w93>.

[21] K. Bharti, A. Cervera-Lierta, T. H. Kyaw, T. Haug, S. Alperin-Lea, A. Anand, M. Degroote, H. Heimonen, J. S. Kottmann, T. Menke, et al., *Rev. Mod. Phys.* **94**, 015004 (2022), URL <https://link.aps.org/doi/10.1103/RevModPhys.94.015004>.

[22] A. Morvan, V. V. Ramasesh, M. S. Blok, J. M. Kreikebaum, K. O'Brien, L. Chen, B. K. Mitchell, R. K. Naik, D. I. Santiago, and I. Siddiqi, *Physical review letters* **126**, 210504 (2021).

[23] N. Goss, A. Morvan, B. Marinelli, B. K. Mitchell, L. B. Nguyen, R. K. Naik, L. Chen, C. Jünger, J. M. Kreikebaum, D. I. Santiago, et al., *Nature communications* **13**, 7481 (2022).

[24] Y. Sung, A. Vepsäläinen, J. Braumüller, F. Yan, J. I.-J. Wang, M. Kjaergaard, R. Winik, P. Krantz, A. Bengtsson, A. J. Melville, et al., *Nature communications* **12**,

967 (2021).

[25] M. Ringbauer, M. Meth, L. Postler, R. Stricker, R. Blatt, P. Schindler, and T. Monz, *Nature Physics* **18**, 1053 (2022).

[26] I. V. Zalivako and et al., *Quantum Reports* **7** (2025), ISSN 2624-960X, URL <https://www.mdpi.com/2624-960X/7/2/19>.

[27] Y. Fu, W. Liu, X. Ye, Y. Wang, C. Zhang, C.-K. Duan, X. Rong, and J. Du, *Physical Review Letters* **129**, 100501 (2022).

[28] H. Zhou, H. Gao, N. T. Leitao, O. Makarova, I. Cong, A. M. Douglas, L. S. Martin, and M. D. Lukin, *Physical Review X* **14**, 031017 (2024).

[29] I. Fernández de Fuentes, T. Botzem, M. A. Johnson, A. Vaartjes, S. Asaad, V. Mourik, F. E. Hudson, K. M. Itoh, B. C. Johnson, A. M. Jakob, et al., *Nature communications* **15**, 1380 (2024).

[30] D. González-Cuadra, T. V. Zache, J. Carrasco, B. Kraus, and P. Zoller, *Phys. Rev. Lett.* **129**, 160501 (2022), URL <https://link.aps.org/doi/10.1103/PhysRevLett.129.160501>.

[31] R. Sawant, J. A. Blackmore, P. D. Gregory, J. Mur-Petit, D. Jaksch, J. Aldegunde, J. M. Hutson, M. R. Tarbutt, and S. L. Cornish, *New Journal of Physics* **22**, 013027 (2020).

[32] K.-K. Ni, S. Ospelkaus, M. De Miranda, A. Pe'Er, B. Neyenhuis, J. Zirbel, S. Kotochigova, P. Julienne, D. Jin, and J. Ye, *science* **322**, 231 (2008).

[33] J. Deiglmayr, A. Grochola, M. Repp, K. Mörtlbaumer, C. Glück, J. Lange, O. Dulieu, R. Wester, and M. Weidmüller, *Physical review letters* **101**, 133004 (2008).

[34] S. Ospelkaus, K.-K. Ni, D. Wang, M. De Miranda, B. Neyenhuis, G. Quéméner, P. Julienne, J. Bohn, D. Jin, and J. Ye, *Science* **327**, 853 (2010).

[35] K.-K. Ni, S. Ospelkaus, D. Wang, G. Quéméner, B. Neyenhuis, M. De Miranda, J. Bohn, J. Ye, and D. Jin, *Nature* **464**, 1324 (2010).

[36] M. De Miranda, A. Chotia, B. Neyenhuis, D. Wang, G. Quéméner, S. Ospelkaus, J. Bohn, J. Ye, and D. Jin, *Nature Physics* **7**, 502 (2011).

[37] L. D. Carr, D. DeMille, R. V. Krems, and J. Ye, *New Journal of Physics* **11**, 055049 (2009).

[38] D. DeMille, *Physical Review Letters* **88**, 067901 (2002).

[39] P. D. Gregory, J. A. Blackmore, S. L. Bromley, J. M. Hutson, and S. L. Cornish, *Nature Physics* **17**, 1149 (2021).

[40] L. R. Picard, A. J. Park, G. E. Patenotte, S. Gebretsadkan, D. Wellnitz, A. M. Rey, and K.-K. Ni, *Nature* **637**, 821 (2025).

[41] K.-K. Ni, T. Rosenband, and D. D. Grimes, *Chemical science* **9**, 6830 (2018).

[42] Y. Bao, S. S. Yu, L. Anderegg, E. Chae, W. Ketterle, K.-K. Ni, and J. M. Doyle, *Science* **382**, 1138 (2023).

[43] D. Mitra, K. Leung, and T. Zelevinsky, *Physical Review A* **105**, 040101 (2022).

[44] E. R. Hudson, H. Lewandowski, B. C. Sawyer, and J. Ye, *Physical review letters* **96**, 143004 (2006).

[45] T. Zelevinsky, S. Kotochigova, and J. Ye, *Physical review letters* **100**, 043201 (2008).

[46] D. DeMille, S. Sainis, J. Sage, T. Bergeman, S. Kotochigova, and E. Tiesinga, *Physical review letters* **100**, 043202 (2008).

[47] B. Sauer, H. Ashworth, J. Hudson, M. Tarbutt, and E. Hinds, in *AIP conference proceedings* (American Institute of Physics, 2006), vol. 869, pp. 44–51.

[48] A. C. Vutha, O. K. Baker, W. C. Campbell, D. DeMille, J. M. Doyle, G. Gabrielse, Y. V. Gurevich, and M. A. Jansen, in *APS Division of Atomic, Molecular and Optical Physics Meeting Abstracts* (2008), vol. 39, pp. OPC-50.

[49] M. Hughes, M. D. Frye, R. Sawant, G. Bhole, J. A. Jones, S. L. Cornish, M. Tarbutt, J. M. Hutson, D. Jaksch, and J. Mur-Petit, *Physical Review A* **101**, 062308 (2020).

[50] F. Herrera, Y. Cao, S. Kais, and K. B. Whaley, *New Journal of Physics* **16**, 075001 (2014).

[51] E. S. Shuman, J. F. Barry, and D. DeMille, *Nature* **467**, 820 (2010).

[52] L. Anderegg, L. W. Cheuk, Y. Bao, S. Burchesky, W. Ketterle, K.-K. Ni, and J. M. Doyle, *Science* **365**, 1156 (2019).

[53] D. K. Ruttley, A. Guttridge, S. Spence, R. C. Bird, C. R. Le Sueur, J. M. Hutson, and S. L. Cornish, *Physical Review Letters* **130**, 223401 (2023).

[54] F. Luis, P. J. Alonso, O. Roubeau, V. Velasco, D. Zueco, D. Aguilà, J. I. Martínez, L. A. Barrios, and G. Aromí, *Communications Chemistry* **3**, 176 (2020).

[55] A. Hernández-Antón, F. Luis, and A. Castro, *Optimal control of spin qudits subject to decoherence using amplitude-and-frequency-constrained pulses* (2024), 2403.15785, URL <https://arxiv.org/abs/2403.15785>.

[56] L. D. Landau and E. M. Lifshitz, *Quantum mechanics: non-relativistic theory*, vol. 3 (Elsevier, 2013).

[57] W. Ernst, J. Kändler, S. Kindt, and T. Törring, *Chemical physics letters* **113**, 351 (1985).

[58] Y. Hao, L. F. Pašteka, L. Visscher, P. Aggarwal, H. L. Bethlehem, A. Boeschoten, A. Borschovsky, M. Denis, K. Esajas, S. Hoekstra, et al., *The Journal of chemical physics* **151** (2019).

[59] P. K. Molony, P. D. Gregory, Z. Ji, B. Lu, M. P. Köppinger, C. R. Le Sueur, C. L. Blackley, J. M. Hutson, and S. L. Cornish, *Physical review letters* **113**, 255301 (2014).

[60] S. Burchesky, L. Anderegg, Y. Bao, S. S. Yu, E. Chae, W. Ketterle, K.-K. Ni, and J. M. Doyle, *Physical Review Letters* **127**, 123202 (2021).

[61] R. Bause, M. Li, A. Schindewolf, X.-Y. Chen, M. Duda, S. Kotochigova, I. Bloch, and X.-Y. Luo, *Physical Review Letters* **125**, 023201 (2020).

[62] J. A. Blackmore, R. Sawant, P. D. Gregory, S. L. Bromley, J. Aldegunde, J. M. Hutson, and S. L. Cornish, *Physical Review A* **102**, 053316 (2020).

[63] F. Seefelberg, X.-Y. Luo, M. Li, R. Bause, S. Kotochigova, I. Bloch, and C. Gohle, *Physical Review Letters* **121**, 253401 (2018).

[64] J. Lin, J. He, X. Ye, and D. Wang, *Physical Review A* **103**, 023332 (2021).

[65] B. Neyenhuis, B. Yan, S. Moses, J. Covey, A. Chotia, A. Petrov, S. Kotochigova, J. Ye, and D. Jin, *Physical review letters* **109**, 230403 (2012).

[66] C. P. Williams and C. P. Williams, *Explorations in quantum computing* pp. 51–122 (2011).

[67] A. S. Nikolaeva, E. O. Kiktenko, and A. K. Fedorov, *Physical review A* **105**, 032621 (2022).

[68] A. S. Nikolaeva, E. O. Kiktenko, and A. K. Fedorov, *EPJ Quantum Technology* **11**, 1 (2024).